Supplementary figures

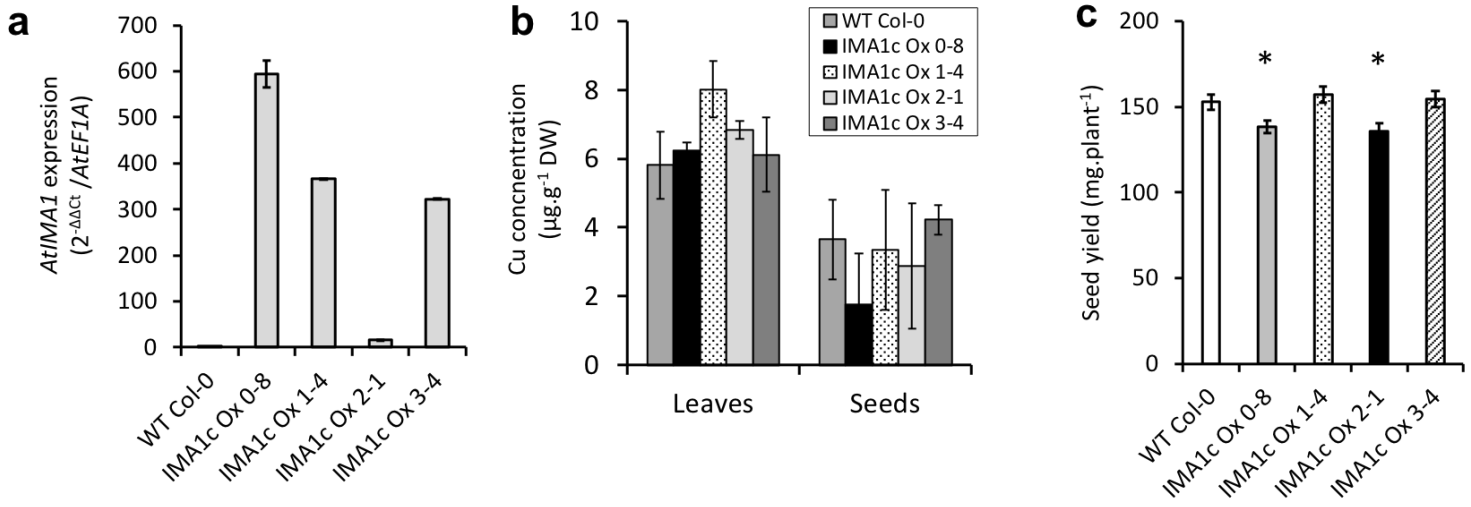

Figure S1. Characterization of IMA1 Ox (*35Spro::AtIMA1*$_{cDNA}$*)* lines. (a) Expression level of *AtIMA1*. (b) Cu quantification. (c) seed yield.

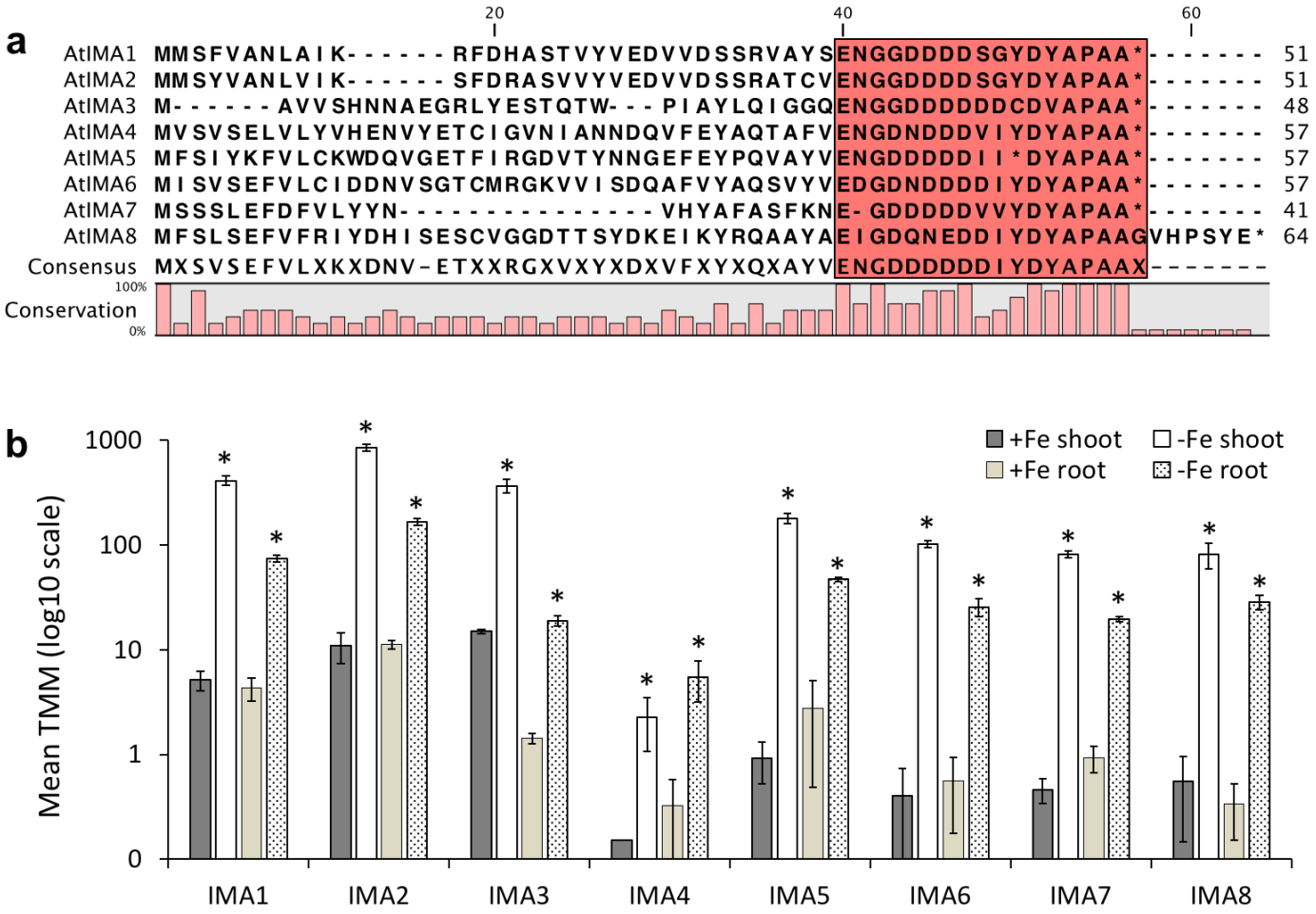

Figure S2: Identification of Arabidopsis IMA genes and their Fe-deficiency regulation. (a) Alignment of putative IMA proteins and (b) Expression level of the 8 Arabidopsis IMA genes in Fe-sufficient and Fe-deficient leaves and roots. TMM values were calculated using reanalyzed data from (*11*) and (*35*), stars indicate statistical differences to plants grown on control media (Z-Test).

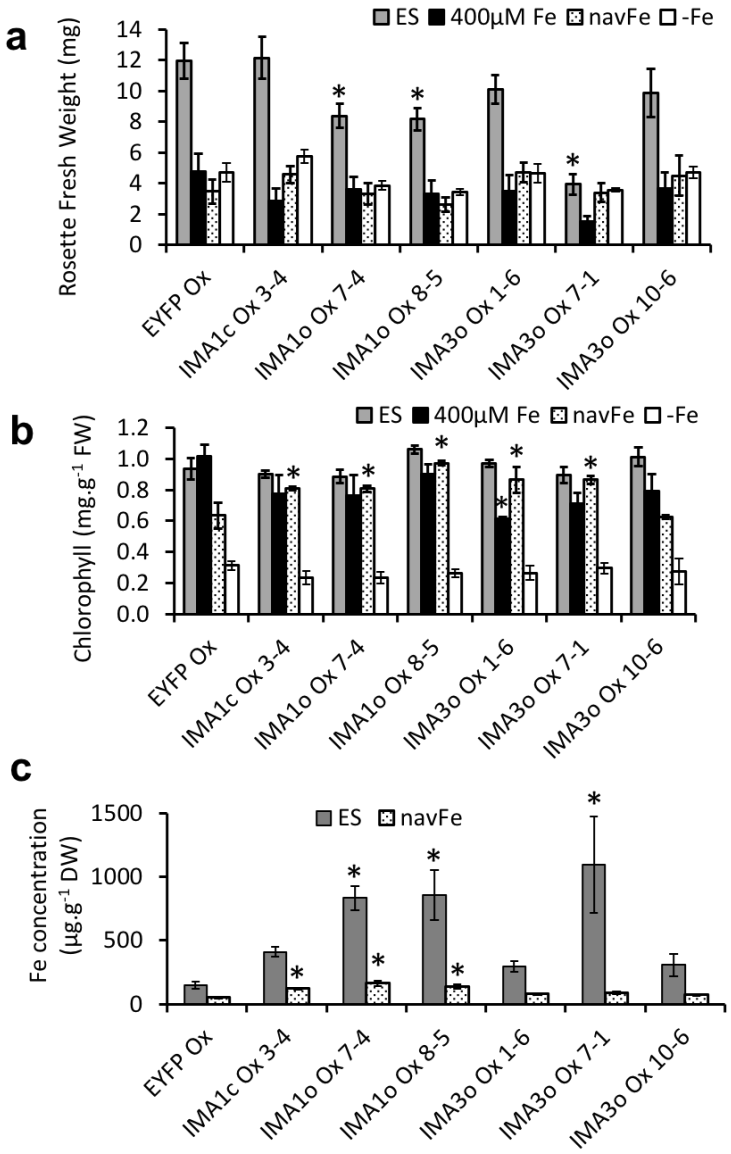

Figure S3. Characterization of IMA1 Ox and IMA3 Ox lines**.** (a) Biomass production (n = 3 sets of 25 rosettes) and (b) chlorophyll concentration of 13-day-old IMA1 Ox and IMA3 Ox lines grown under various Fe regimes (n = 6 sets of 5 rosettes). (c) Leaf Fe concentration of plants grown on control or navFe media (n = 6 sets of 15 rosettes). ES, Estelle and Somerville media containing 40 µM FeEDTA; navFe, ES media containing 10 µM $FeCl_3$, pH 7; -Fe, ES media without added Fe supplemented with 100 µM FerroZine (FRZ); IMA1c Ox: 35Spro::At$IMA1_{cDNA}$; IMA1o Ox: 35Spro::At$IMA1_{ORF}$; IMA3o Ox: 35Spro::At$IMA3_{ORF}$. Results show means ± SE. Stars indicate significant difference to control plants grown under the same conditions (Duncan test, $P \leq 0.05$).

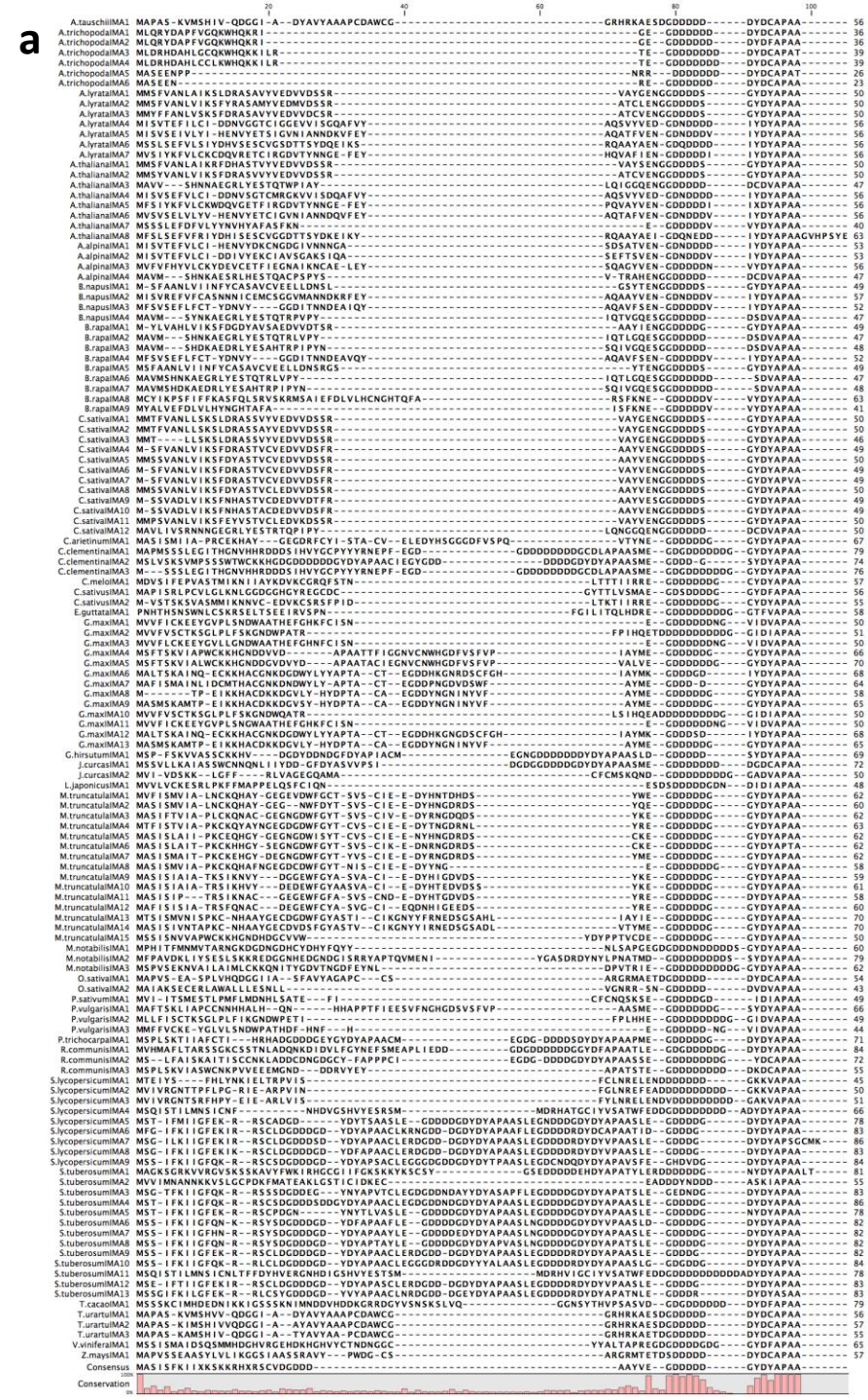

Figure S4. (a) Alignment and consensus plot of 131 amino acid sequences of putative IMAs found by BLAST search of the conserved motif in various EST and genome sequence databases listed in Supplementary Table 2. (b) Phylogenetic neighbour-joining tree inferred from the alignment of the putative IMAs (10000 bootstrap).

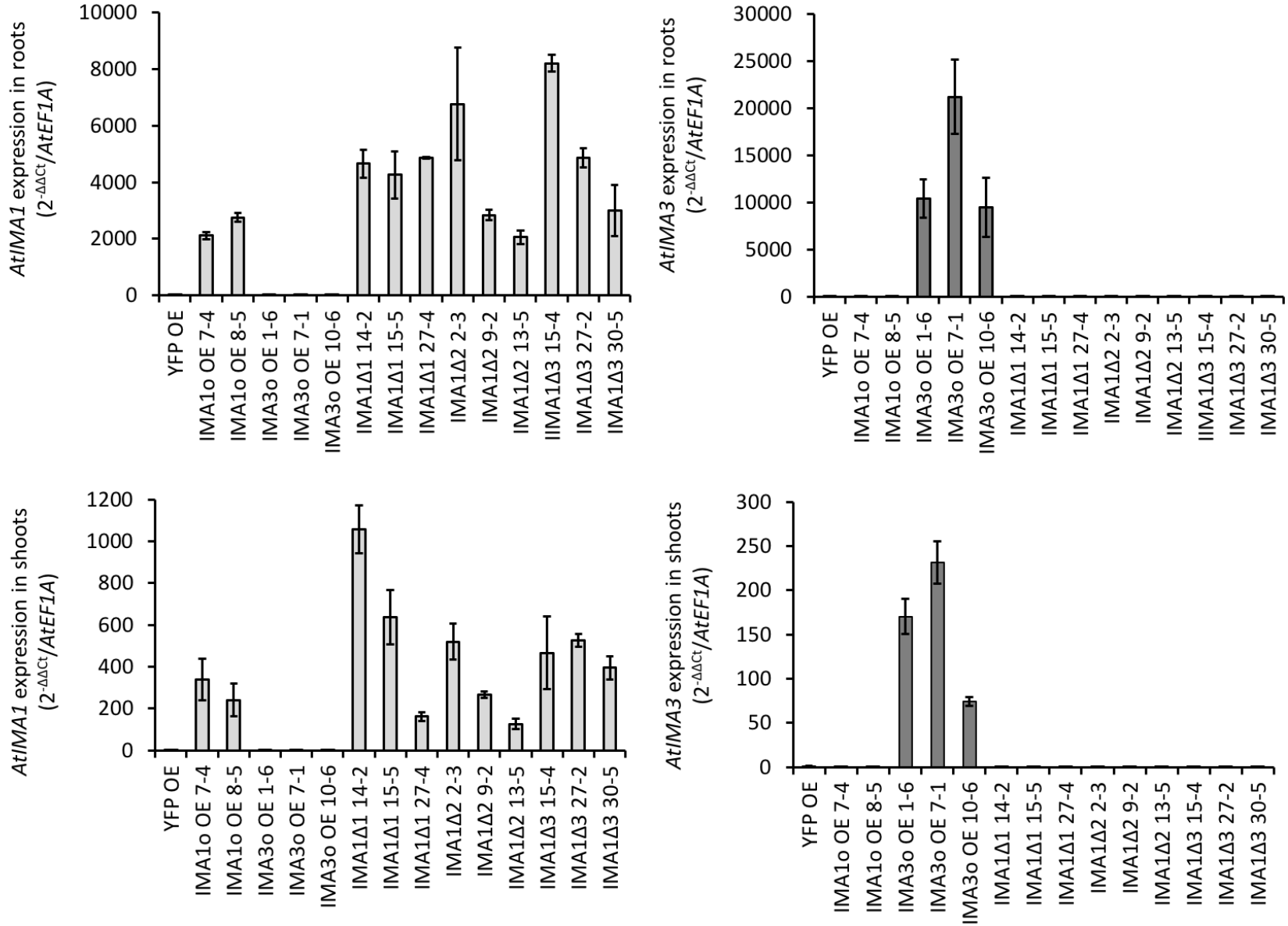

Figure S5. Expression level of *AtIMA1* and *AtIMA3* in roots and leaves of transgenic plants expressing the ORFs of either *AtIMA1*, *AtIMA3,* and mutant versions of *AtIMA1* harboring deletions under the control of the *CaMV 35S* promoter.

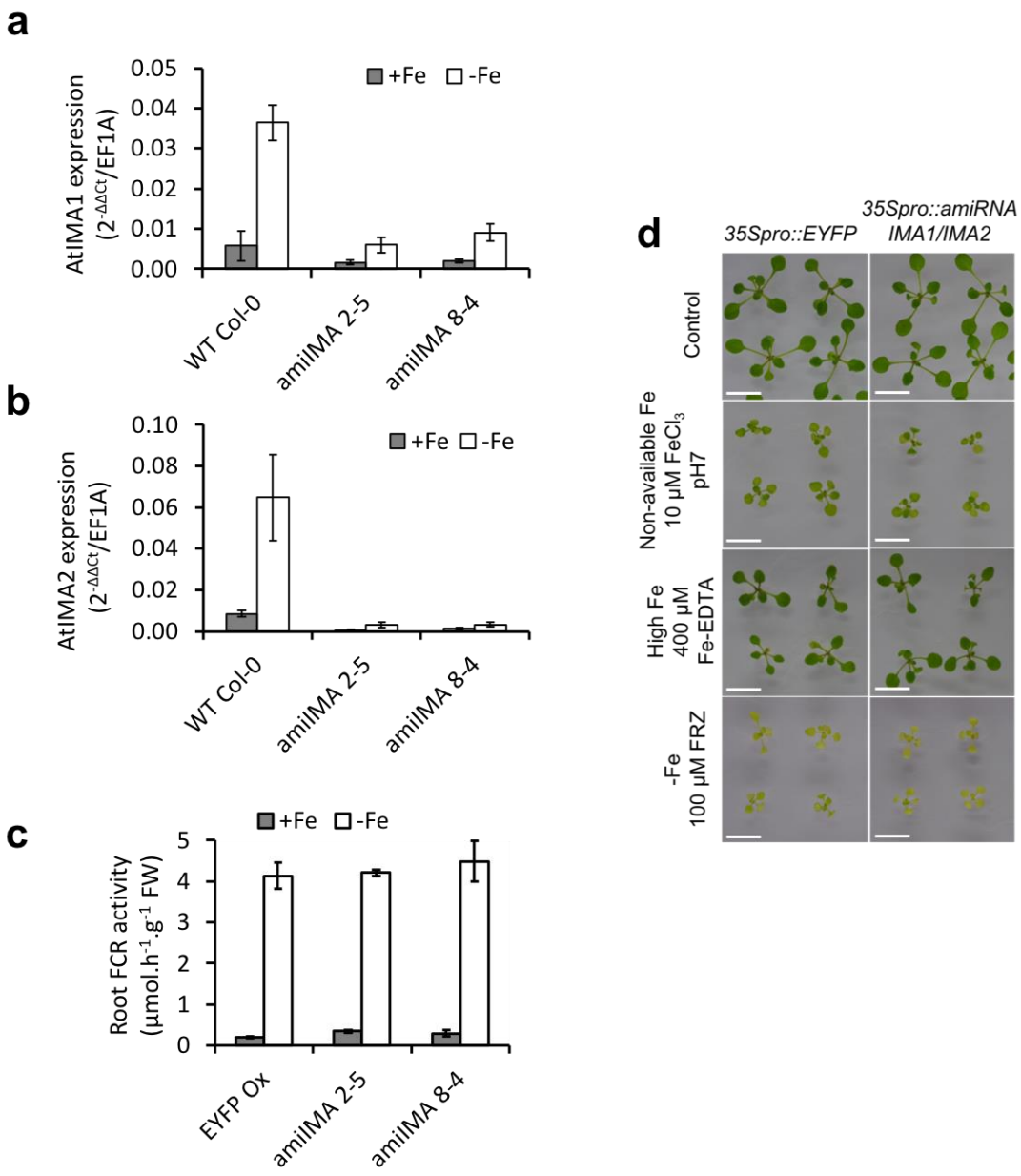

Figure S6: Silencing of AtIMA1 and AtIMA2 using expressing an artificial microRNA targeting both genes. (a) Expression of AtIMA1 and AtIMA2 in Fe-sufficient and Fe-deficient seedlings, (b) root FCR activity and (c) phenotype of the seedlings under various Fe supply.

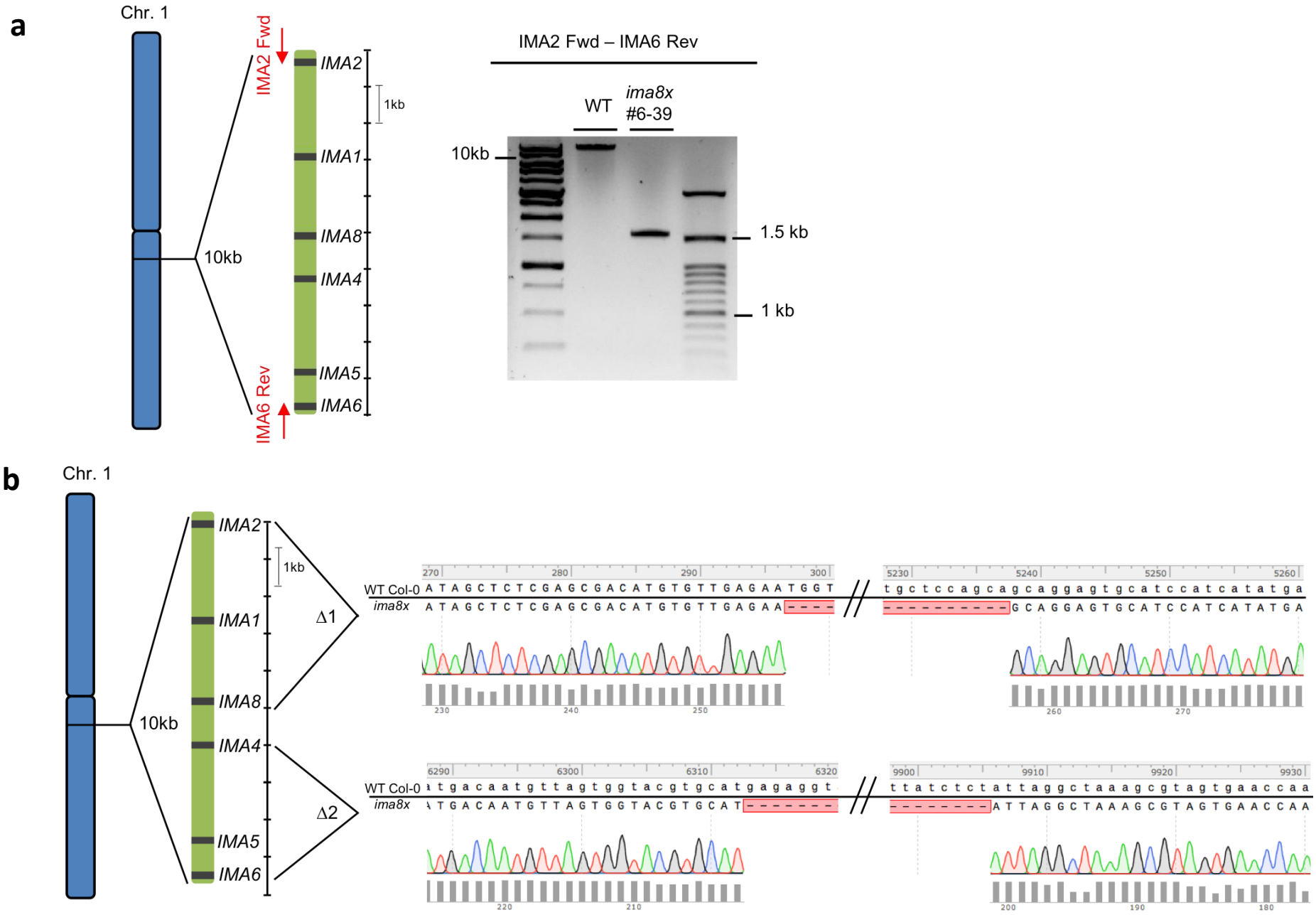

Figure S7. Genotyping of the mutations on chromosome 1 in the *ima8x* mutant line #6-39. (a) PCR of the 10kb region harboring six *IMA* genes. (b) Sequencing of the deletions and alignment with genome sequence of Col-0.

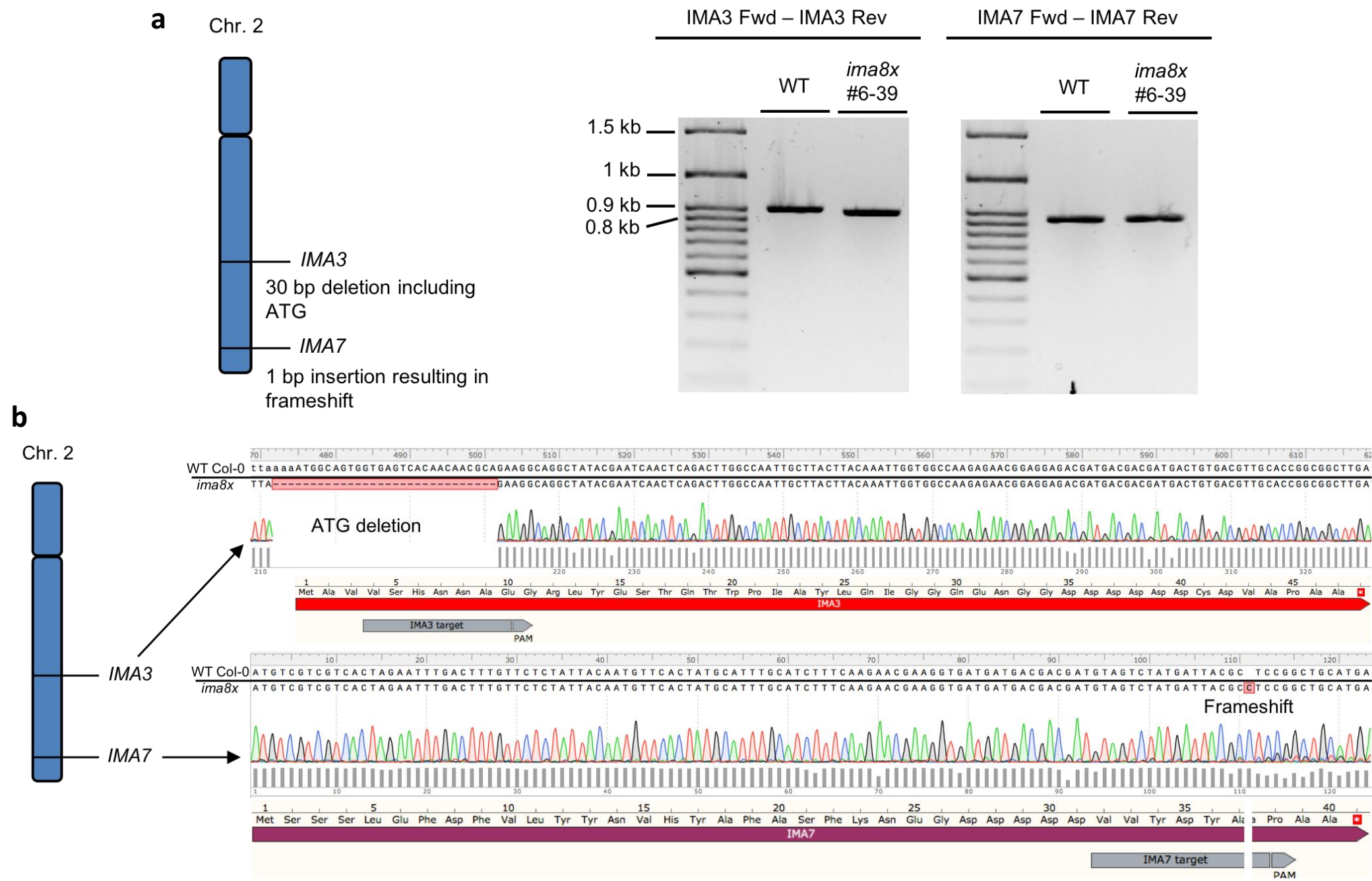

Figure S8. Genotyping of the mutations on chromosome 2 in the *ima8x* mutant line #6-39. (a) PCR amplification of regions harboring either *IMA3 or IMA7* genes. (b) Sequencing of the mutations and alignment with genome sequence of Col-0.

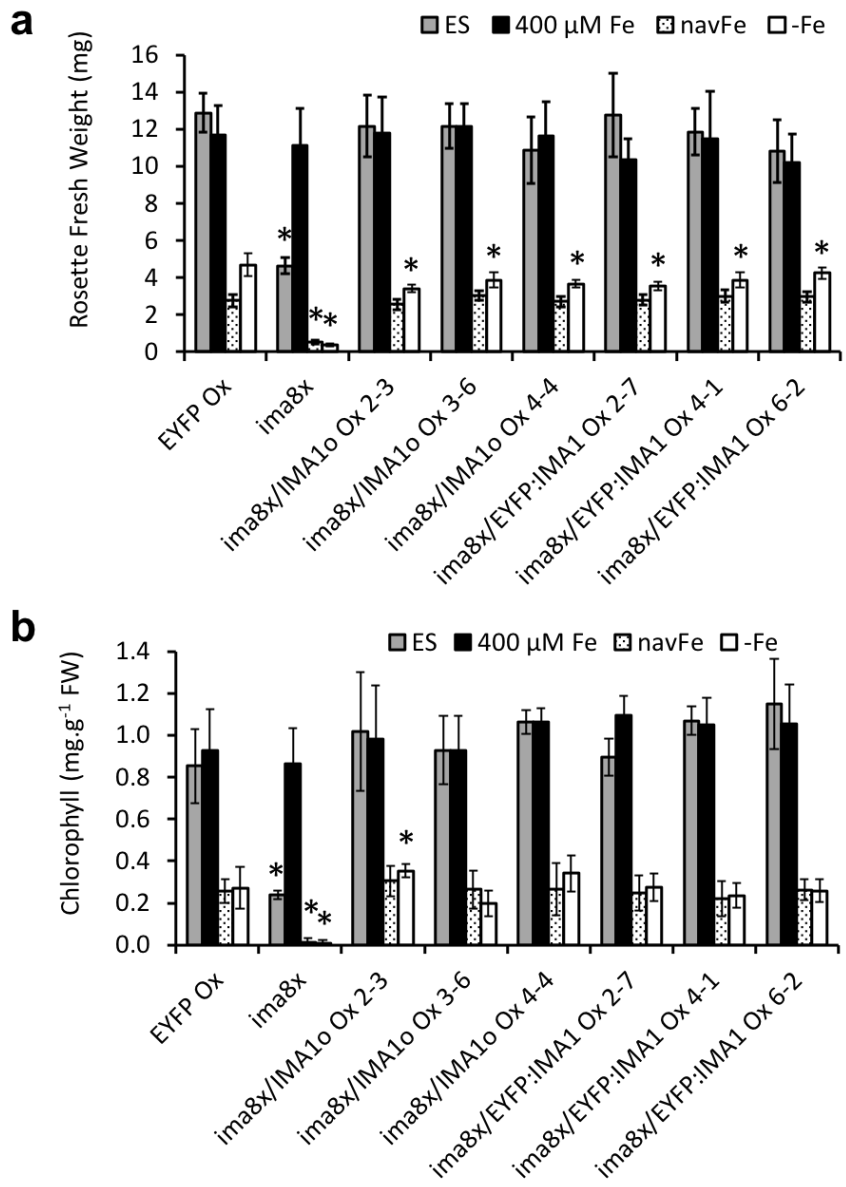

Figure S9. Silencing of eight *IMA* genes by CRISPR-Cas9 gene editing and complementation with *IMA1 and EYFP:IMA1*. (a) Biomass production (n = 3 sets of 25 rosettes). (b) chlorophyll concentration (n = 6 sets of 3 to 8 rosettes). ES, Estelle and Somerville media containing 40 µM FeEDTA; Non-available Fe, ES media containing 10 µM $FeCl_3$, pH 7; -Fe, ES media without added Fe supplemented with 100 µM FerroZine (FRZ).

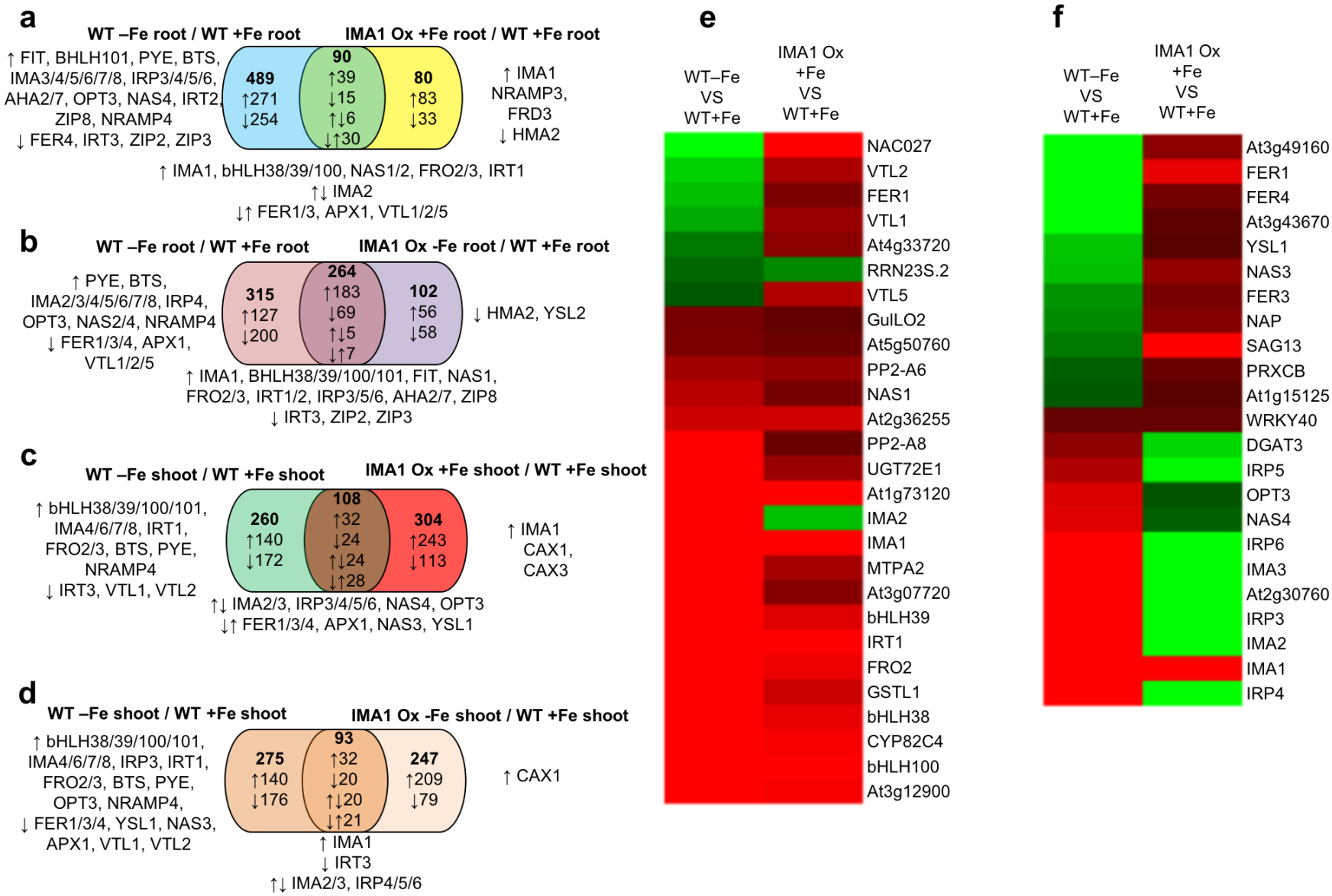

Figure S10. Comparative transcriptome analysis of IMA1 Ox lines grown on Fe-replete (+Fe) and Fe-free (-Fe) media. (a-d) Venn diagrams showing DEGs in wild-type and IMA1 Ox plants. Upward arrows indicate upregulated genes; downward arrows denote downregulated genes. Gene symbols preceded by oppositely oriented arrows indicate genes that are regulated differently in the two genotypes. DEGs denoted in blue were upregulated in Fe-deficient wild-type and down-regulated in IMA1 Ox and DEGs shown in purple were downregulated in wild-type and upregulated in IMA1 Ox. (e, f) Expression changes of the overlapping most differentially expressed genes between IMA1 Ox and control plants (log2 FC > 1) in roots (e) and leaves (f). Data for the wild type are taken from[11] and[35]. All DEGs are listed in Supplementary Dataset 1.

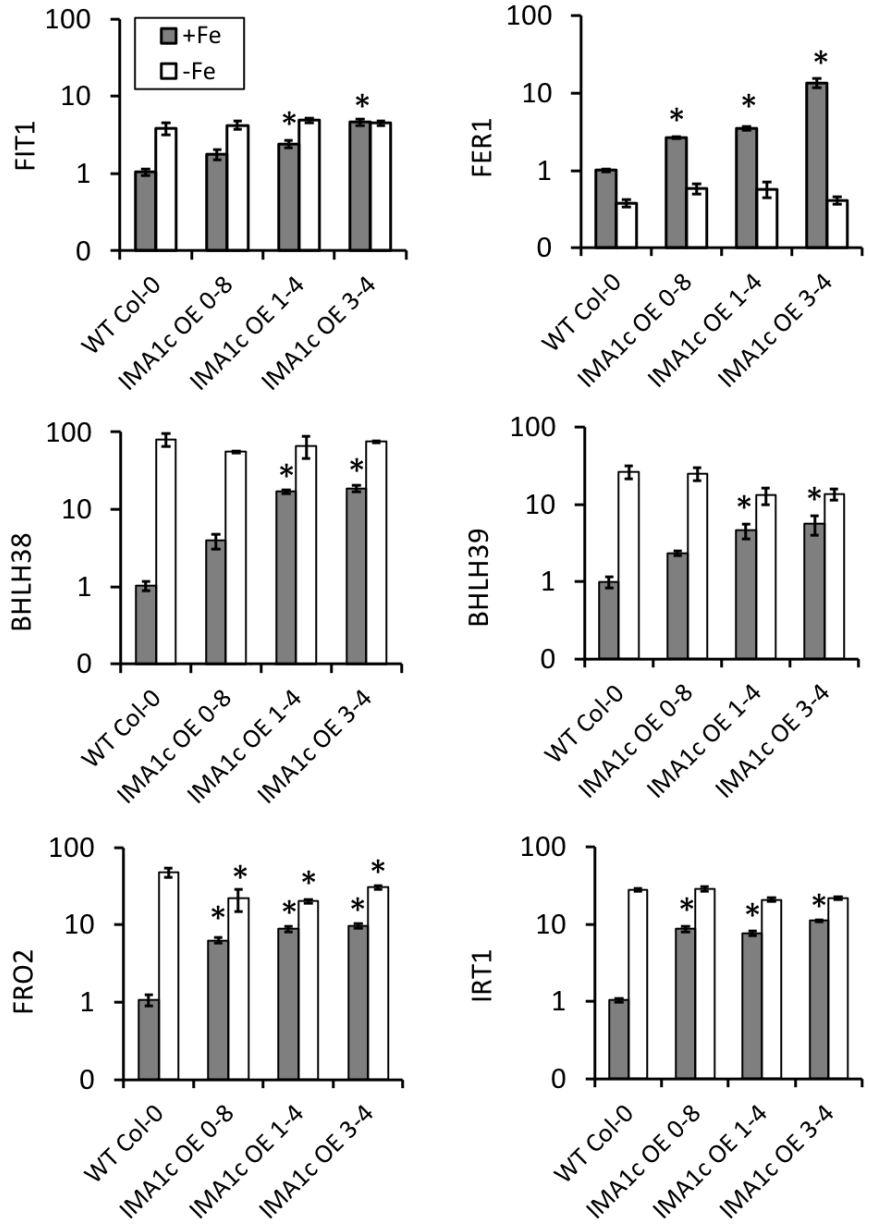

Figure S11. Analysis of *FIT*, *FER1*, *BHLH38*, *BHLH39*, *FRO2* and *IRT1* gene expression in roots of Fe-replete and Fe-deficient IMA1 Ox (35Spro::AtIMA1cDNA) seedlings. Data are expressed relative to Fe-replete wild-type plants as $2^{-\Delta\Delta Ct}$ using EF1α as a reference gene.

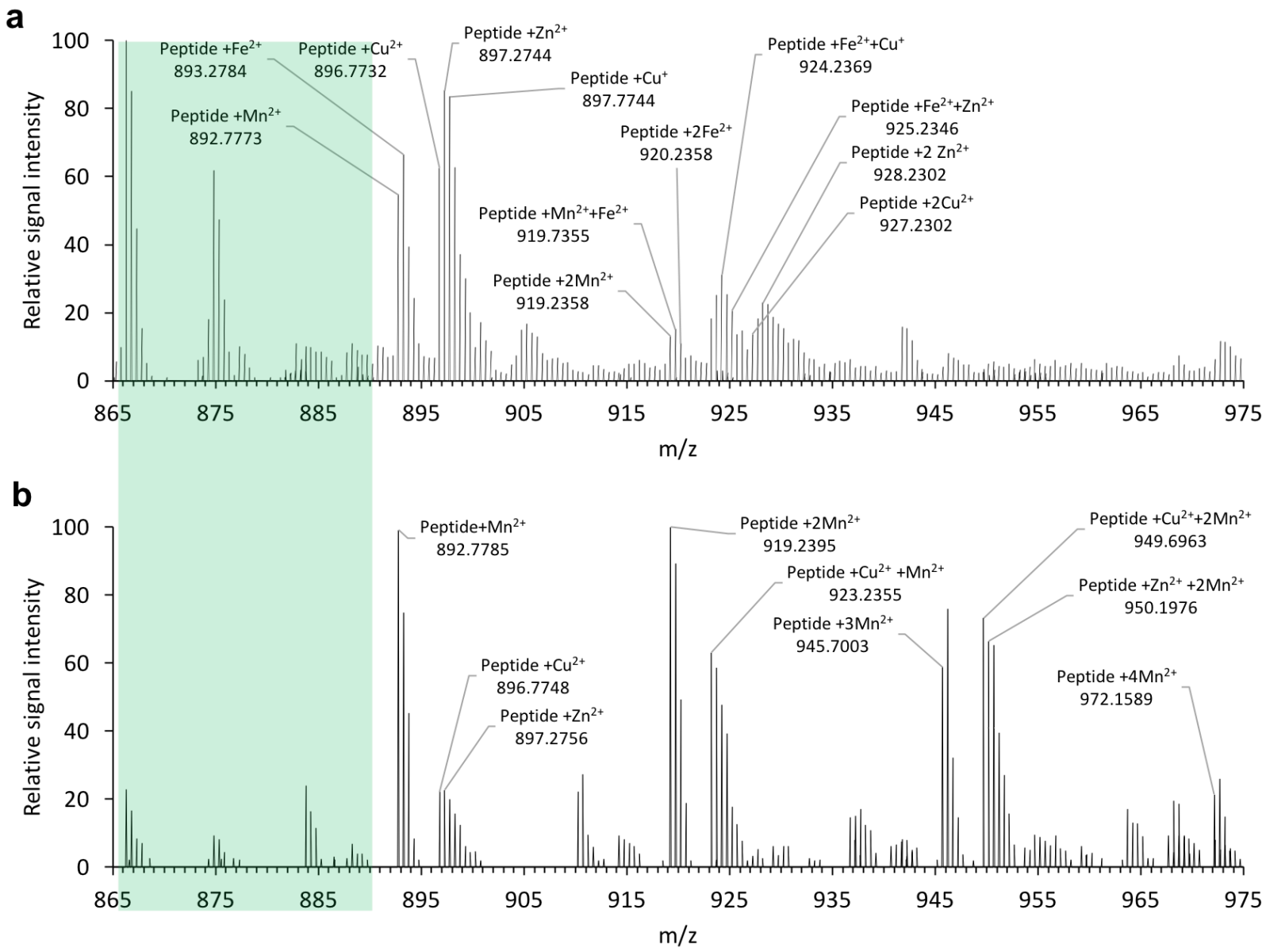

Figure S12. ESI-MS spectra of the IMA1 C-term synthetic peptide in a solution consisting of 100 µM Fe, 100 µM Zn, 100 µM Cu, and 100 µM Mn buffered at pH5 with 10 mM ammonium acetate in the presence (upper chart) or absence (lower chart) of ascorbic acid. *m/z* ratios of peaks corresponding to the ligand-free peptide are indicated by green colour. Peaks corresponding to peptide complexes with ^{56}Fe, ^{63}Cu, ^{64}Zn, and ^{55}Mn have been annotated.

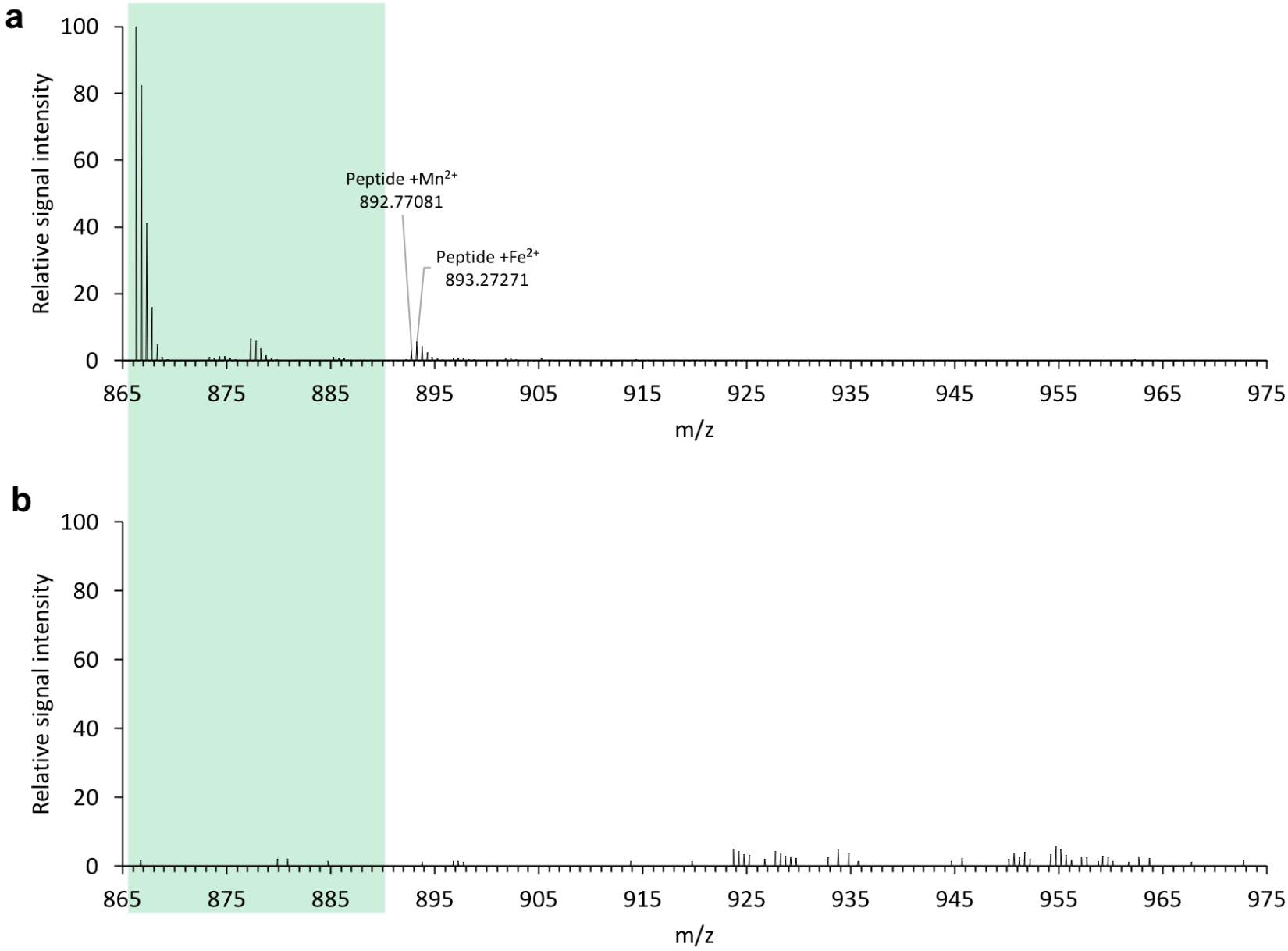

Figure S13. ESI-MS spectra of the IMA1 C-term synthetic peptide. (a) Spectrum obtained after liquid chromatography using acetonitrile with 0.1% formic acid and (b) after addition of 500 µM Fe, 500 µM Zn, 500 µM Cu, and 500 µM Mn buffered at pH5 with 10 mM ammonium acetate in the presence of ascorbic acid. *m/z* ratios of peaks corresponding to the ligand-free peptide are indicated by green colour.

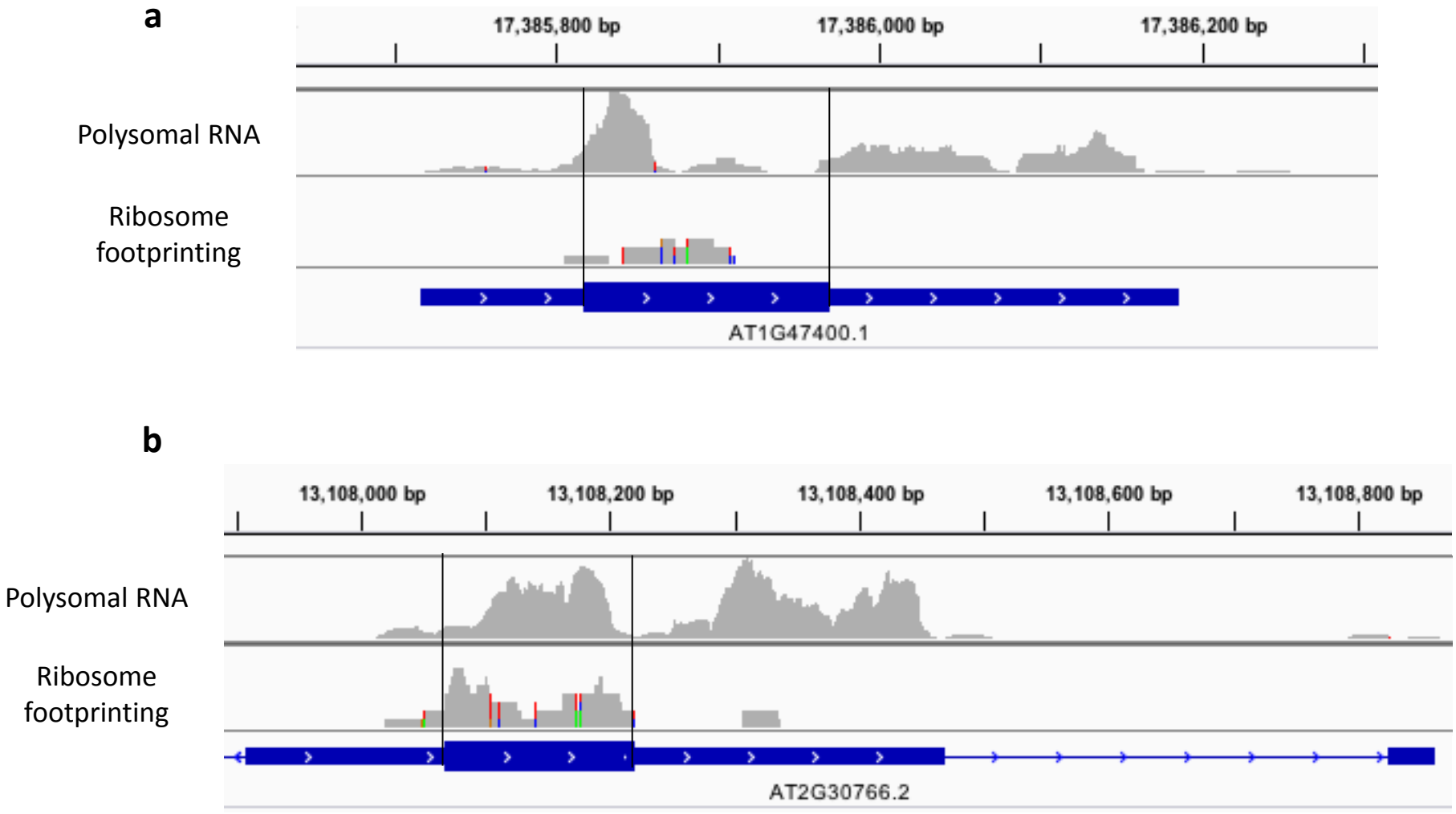

Figure S14. Translation of IMA genes. aligned reads of *AtIMA1* (a) and *AtIMA3* (b) derived from RNA sequencing of gradient-purified polysomal RNA and ribosome-protected RNA. Data are a courtesy of Dr. Bailey-Serres taken from[50]. *AtIMA1* and *AtIMA3* mRNAs are associated to polysomes. Reads matching the ORFs are enriched in the ribosome-protected RNA compared to polysomal RNA.